Strain-Induced Crystallization in Uniaxially Drawn PETG Plates

M. KATTAN,[1,2] E. DARGENT,[1] J. LEDRU,[1] J. GRENET[1]

[1] Laboratoire d'Etude et de Caractérisation des Amorphes et des Polymères, Université de Rouen, Faculté des Sciences, 76821 Mont-Saint-Aignan Cedex, France

[2] AECS Damascus, P.O. Box 6091, Syria

Received 3 October 2000; accepted 29 November 2000

ABSTRACT: The copolyester poly(ethylene glycol-*co*-cyclohexane-1,4-dimethanol terephthalate) (PETG) is used industrially as an uncrystallizable polymer, whereas PET is an inherently crystallizable polymer. Nevertheless, a crystalline phase could appear in the material. To create a strain-induced crystalline phase in an initially amorphous PETG material, plates were placed in the heating chamber of a tensile machine at 100°C and uniaxially drawn to obtain different samples with various draw ratios. During DSC analysis of highly drawn samples, perturbations of the baseline appear above the glass-transition temperature, consisting of weak exothermic and endothermic phenomena. Comparison of DSC and X-ray diffraction analysis of drawn PETG and PET shows that a strain-induced crystalline phase appears in this copolyester. A spherulitic superstructure could also appear after lengthy annealing. Analysis of this semicrystalline material allowed estimation of the degree of crystallinity, about 3% after a drawing at high draw ratio and about 11% for undrawn annealed material. © 2001 John Wiley & Sons, Inc. J Appl Polym Sci 81: 3405–3412, 2001

Key words: PETG; crystalline phase; strain-induced crystallization; copolyester; PET

INTRODUCTION

Numerous companies manufacture poly(ethylene terephthalate) (PET) resin, which is an inherently crystallizable polymer. PET is also one of the most studied polymers because the recrystallization of the glassy amorphous material could be obtained either by thermal treatment, which leads to an isotropic structure, or by drawing, which gives an anisotropic structure. PET is widely used in fibers, films, and bottles and during the forming process it generally appears a strain-induced crystallized (SIC) phase. Previous studies on PET focused on the phenomenon of strain-induced crystallization.[1–5] Moreover, characterizations of the noncrystalline phase of drawn PET showed the appearance of a highly oriented amorphous phase, which served as the precursor for extended chain crystallization.[6]

By replacing some of the ethylene glycol with secondary glycols, the crystallization of the polyester can be slowed down. With a sufficient amount of CHDM (cyclohexane-1,4-dimethanol) added, poly(ethylene glycol-*co*-cyclohexane-1,4-dimethanol terephthalate) (PETG) can be obtained. This material is industrially used as an amorphous copolyester, which is not able to crystallize. PETG offers a range of processing parameters broader than that of normal crystallizable

Correspondence to: E. Dargent (E-mail: eric.dargent@univ-rouen.fr).

Journal of Applied Polymer Science, Vol. 81, 3405–3412 (2001)

polymers and is very useful, especially for obtaining high-clarity amorphous molding.[7] In PETG/poly(butylene terephthalate) (PBT) blends, the retardation in crystallization rate has been attributed to the miscibility in the molten state and the hindrance to the diffusion of crystallizable units of PBT.[8] At low PBT levels, melt-mixed PETG/PBT blends show good mechanical properties that result in an amorphous matrix reinforcement by PBT crystallites.[9] Nevertheless, Radhakrishnan and Nadkarni[10] showed that a crystalline phase could appear in PETG after thermal and solvent treatment. Recently, a thermal analysis of PETG/liquid crystalline copolyester (LCP) blends suggested that LCP can act as a nucleating agent for the crystallization of PETG.[11]

Thus it appears that PETG can crystallize under certain conditions, although strain-induced crystallization has not yet been formally demonstrated. In this work, we try to characterize uniaxially drawn PETG films by differential scanning calorimetry (DSC) and X-ray diffraction (XRD) to know whether a strain-induced crystallized phase could appear in this copolyester.

EXPERIMENTAL

PETG (6763 from Tennessee Eastman Co.) is an amorphous copolymer with $\overline{M_n} \cong 26{,}000$ g/mol. It consists of cyclohexane dimethanol, ethylene glycol, and terephthalic acid with a molar ratio of approximately 1 : 2 : 3. PETG plates ($4 \times 4 \times 0.2$ cm^3) were obtained from pellets by injection molding. To compare PETG and PET, we used isotropic and amorphous PET films ($\overline{M_n} \cong 31{,}000$ g/mol). Dry PETG and PET materials were obtained after drying at room temperature in a vacuum dessiccator in the presence of P_2O_5 until a constant weight was obtained (over a period of 5 days).

Before the drawing period, the plates were placed in the heating chamber of a tensile machine at 100°C for 15 min to allow a homogenous temperature distribution. Plates were then uniaxially drawn at a strain rate of 0.28 s^{-1} in the tensile machine Instron 4301. The drawing temperature was chosen above the glass-transition temperature to allow homogeneous drawing. After drawing, the material was cold-air quenched to room temperature to freeze in its structural state. Finally, different samples were cut from the drawn materials and the draw ratio λ, equal to the ratio of the extended length over the original length, was measured. It was found that λ varies from 1 to 6.4.

Enthalpic analyses were performed with the help of a Perkin–Elmer DSC7 apparatus (Perkin–Elmer Cetus, Norwalk, CT). Calibration was achieved from the determination of the temperature and the enthalpy of fusion of indium and zinc. Calorimetric measurements were made under nitrogen with a heating rate of 10°C/min and the DSC curves were normalized to 1 mg of matter. XRD was performed with a wide-angle X-ray scattering apparatus, a Siemens D5000 goniometer (Siemens Medical Systems, South Iselin, NJ), functioning at 40 kV and 30 mA and using Fe-filtered CoK_α radiation. The reflection procedure was used to obtain the scattered intensity versus 2θ, where θ is the angle between the incident beam and a reference axis parallel to the surface of the sample. Optical observation was performed with a Nikon Optiphot-2 microscope equipped with polarizing plates and with a Mettler FP82 HT heating chamber (temperature controlled by a central Mettler FP90).

RESULTS AND DISCUSSION

Between 70 and 85°C, DSC analysis of an undrawn PETG sample ($\lambda = 1$; Fig. 1) shows the glass transition defined by the onset temperature T_g. As for other wholly amorphous thermoplastics, this transition is the sole observable thermal phenomenon in the scanned temperatures. Up to $\lambda < 3.5$, the DSC curves of the weakly drawn samples are similar to the DSC curve of undrawn PETG. Above this draw ratio, variations of the glass-transition temperature are no longer observable and the DSC curves show a decrease (down to 29% for $\lambda = 6.4$) of the heat capacity step at the glass transition. Classically, this decrease can be attributed to an increase of the degree of crystallinity (for semicrystalline polymers) and/or to an increase of the "rigid" amorphous fraction.[12] This constrained third phase is unable to participate in the relaxation associated with the normal amorphous phase and revealed by the glass transition. Supplementary thermal phenomena are observable for PETG drawn above $\lambda = 3.5$. Above the glass transition, perturbations of the baseline appear between 95 and 180°C, consisting of weak exothermic and endothermic phenomena.

The enthalpies associated with these phenomena are low (less than 8 J g^{-1} K^{-1}) compared to the thermal phenomena observed for amorphous

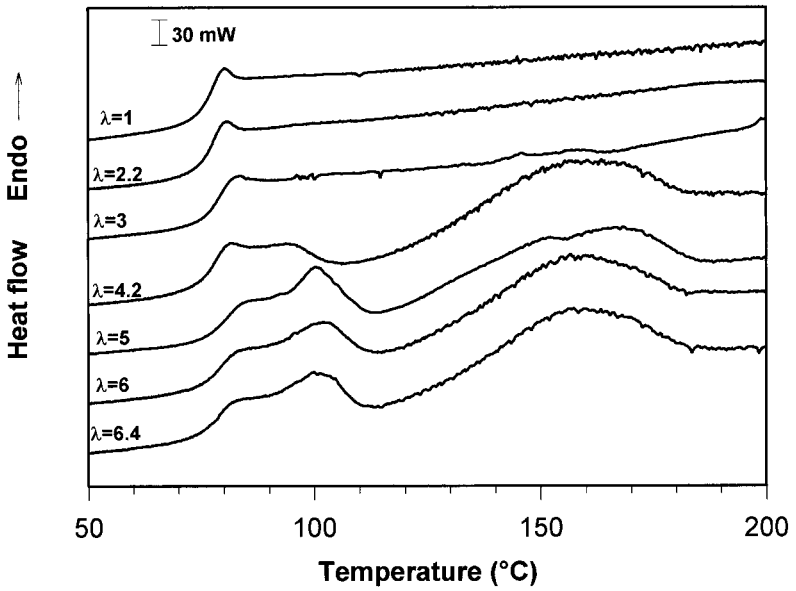

Figure 1 DSC curves for different drawn PETG (λ is the draw ratio).

PET (Fig. 2 and Table I). The DSC curve of the amorphous and undrawn PET sample shows: (1) the glass transition at 70°C $< T_g <$ 80°C, (2) the thermal cold crystallization peak at 130°C $< T_c <$ 160°C, and (3) the melting peak of the crystalline phase at 220°C $< T_f <$ 260°C. As expected, crystallization of a portion of the material is possible during the scan and the rate of crystallization of PET is high. If a highly drawn PETG is heated to 130°C before DSC analysis, the exothermic phenomena disappear and a second weak endothermic peak appears at 146°C (Fig. 3). Thus the first heating, just above 130°C, induced the appearance of a supplementary peak. This phenomenon is similar to that observed for annealed semicrystalline PET: A thermally crystallized PET sample is obtained from an amorphous material in the glassy state by annealing at 120°C for 40 min. As

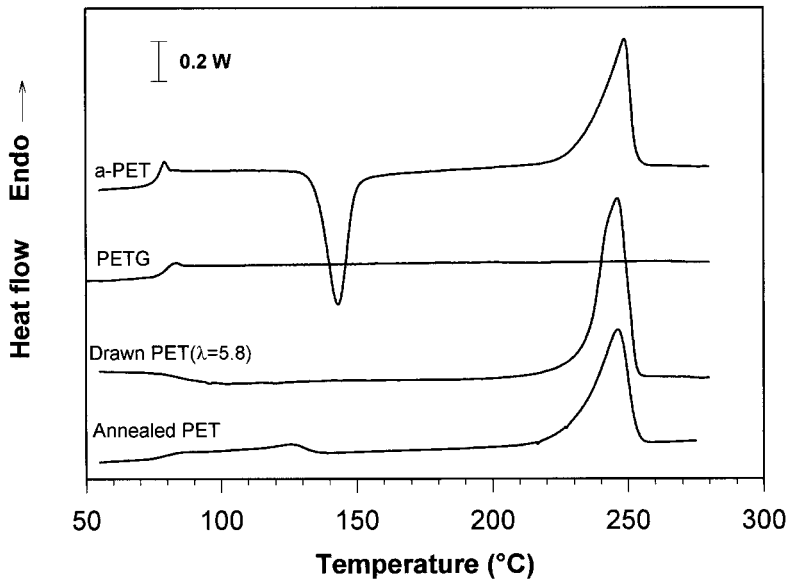

Figure 2 DSC curves for amorphous undrawn PET (a-PET), PETG, drawn PET (λ = 5.8), and annealed PET (at 120°C).

Table I Thermal Properties of PET and PETG

	ΔH_f (J g^{-1} K^{-1})	X_c (%)	X'_c (%)
Amorphous PET	38	0	0
Annealed PET	39	28	27
Drawn PET (λ = 5.8)	54	39	45
Amorphous PETG	0	0	0
Annealed PETG	8		11
Drawn PETG (λ = 6.4)	7.5		18

for annealed semicrystalline polyesters, a supplementary weak endothermic peak can be observed just above the annealing temperature (here at 126°C; Fig. 2). This peak, which depends on the annealing conditions (time, temperature),[13] is attributed to the melting of crystallites formed during the annealing treatment by partial melting and recrystallization mechanism. It could be attributed to crystal thickening[14] as well as to crystal perfection and fold-surface smoothing of the crystalline layers.[15]

Thus comparison of PETG and PET DSC scans leads us to reconsidered the amorphous nature of PETG. In a first hypothesis, the exothermic and the endothermic phenomena may be attributed, respectively, to crystallization and melting peaks. Nevertheless, the magnitude of DSC exo- and endotherms for PETG are well below that for PET. Furthermore, the endothermic peaks appear at quite different temperatures for PET and PETG. So, even if the thermal behavior of annealed drawn PETG favors the possibility that PETG will crystallize, DSC analysis is not sufficient to prove the existence of this crystalline phase in drawn PETG. Moreover, a second explanation is possible: optical microscopic observation with a heating chamber has shown an important thermal shrinkage between 90 and 110°C of a drawn sample. The length in the draw ratio direction decreases by 65%, whereas the length in the perpendicular direction increases by 17%. The total surface of a sample decreases by 60%. It follows that the thermal contact in the DSC oven is modified, thus perturbing the signal. With the help of the microscope, we also observe important modifications of the birefringence between 140 and 170°C. Above this latter temperature, the birefringence becomes negligible. In a first approach the weak DSC phenomena can also be attributed to the thermal shrinkage[16] that occurs in drawn materials when the drawn temperature is reached. This phenomenon is well known in stretch-blow molding of PET preform: the stretching can be retracted by briefly reheating the blown bottle.[17] Nevertheless, the reproducibility of the signal is correct and looks similar, whatever the draw ratio, indicating that this explanation is probably insufficient.

X-ray diffraction (XRD) analysis allows us to obtain the intensity (in counts) versus 2θ (in de-

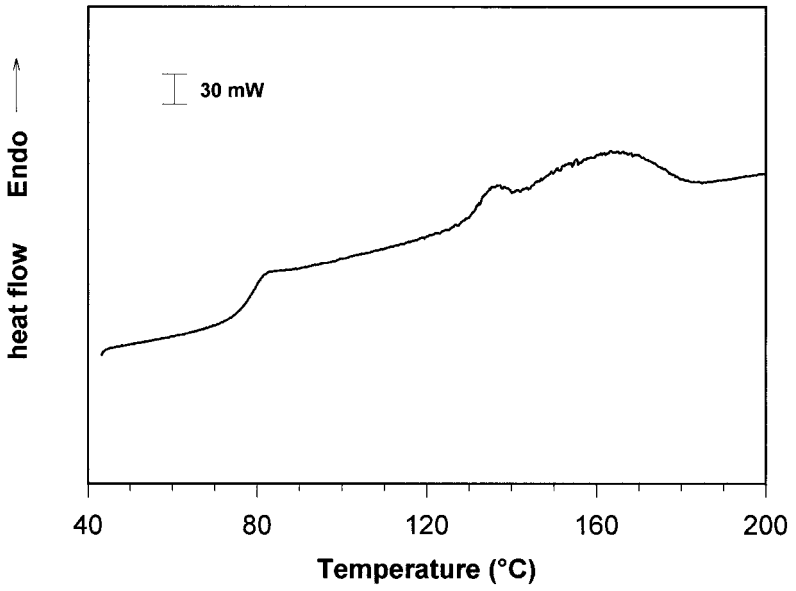

Figure 3 DSC curve for a drawn PETG (λ = 4.6) annealed before DSC scan at 130°C.

grees) and to demonstrate the existence (or not) of a crystalline phase in materials. For the lower values of the draw ratio ($\lambda < 2.8$), the X-ray patterns of drawn PET do not exhibit any peak that could be attributed to the existence of a crystalline phase (Fig. 4). The samples can be considered as amorphous but a gradual growth of the macromolecular orientation can be demonstrated. The polymeric chain-axis becomes parallel to the draw direction.[18,19] The sample crystallizes during the DSC analysis but the recrystallization peak appears in a temperature range below the crystallization temperature range of an undrawn and wholly amorphous sample. Above a critical draw ratio, the SIC phase grows to the detriment of the amorphous phase.[18,20] The XRD analysis of a semicrystalline PET (thermal crystallization) shows (Fig. 5) the three main diffraction peaks at $2\theta = 20$, 26, and 30°, corresponding, respectively, to the planes (010), ($1\bar{1}0$), and (100) of the triclinic lattice structure of crystalline PET.[21] The XRD pattern is quasi-similar for the SIC PET samples.

In principle, it is possible to determine the degree of crystallinity from the relative areas under the crystalline peaks and the amorphous hump for an isotropic structure. Practically, it is difficult to resolve the curve into areas attributed to each phase. Nevertheless, an approximate degree of crystallinity X_c' can be obtained from computer calculations. The contribution of the amorphous phase and the crystalline phase (here, three Gaussian curves) can be computed until the sum of these contributions correctly fits the experimental data (Fig. 5). From the areas we obtain X_c' close to 45 and 27% for the SIC and the thermally crystallized sample, respectively (Table I). In a recent work,[22] we have clearly shown by pole figure and DSC analysis that for the largest

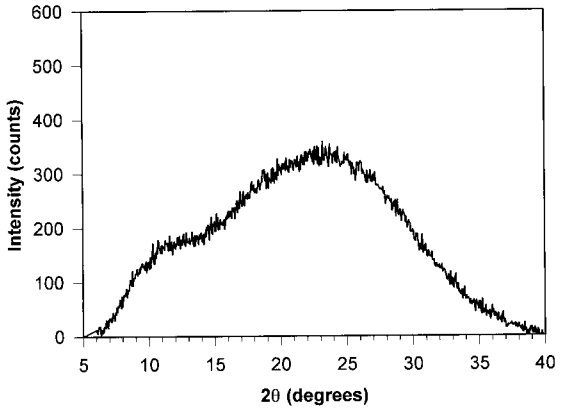

Figure 4 XRD curve for an amorphous PET.

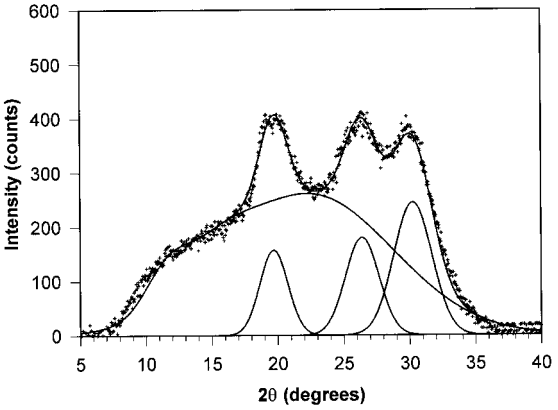

Figure 5 XRD curve for an annealed semicrystalline PET. Data are the plots and the lines correspond to computer calculations.

deformation ratio, there is an alignment of the crystalline structure with the draw direction without modification of the degree of crystallization. As a consequence, the DSC curve does not clearly show any exothermic peak characteristic of crystallization for highly drawn PET samples (Fig. 2).

As for other semicrystalline polymers, a degree of crystallinity X_c can be estimated by DSC from the melting and crystallization peaks using the following equation:

$$X_c = \frac{\Delta H_f - \Delta H_c}{\Delta H_f^\circ} \quad (1)$$

in which ΔH_f is the enthalpy of fusion of a sample (Table I), ΔH_c is the enthalpy of crystallization, and ΔH_f° is the calculated enthalpy of fusion of wholly crystalline PET ($\Delta H_f^\circ = 140$ J/g[23]). The degrees of crystallinity X_c are approximately 39 and 28% for the SIC and the thermally crystallized PET samples, respectively. For isotropic semicrystalline PET, the X_c' value is similar to the value obtained from DSC measurements. Of course, given the texture of the crystalline phase, X_c' is greater than X_c because the explored direction (the direction perpendicular to the drawn direction) is the direction where the dense planes diffract.

For undrawn PETG samples, only the broad hump characteristic of the noncrystalline phases is observed (Fig. 6). That confirms the lack of observations of characteristic peaks of the crystalline phase during the DSC scan of PETG. For weakly drawn PETG samples ($\lambda < 3.5$), no modi-

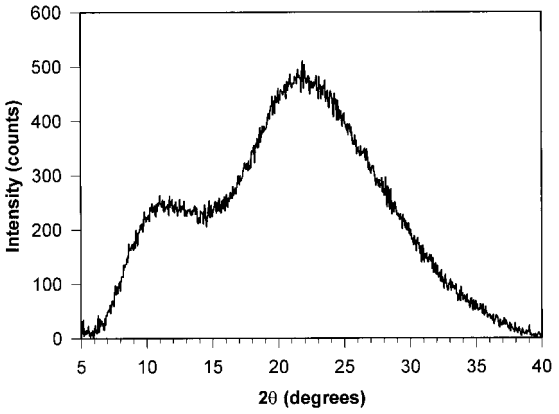

Figure 6 XRD curve for an undrawn PETG.

fication of the XRD patterns is observed, whereas for a high draw ratio ($\lambda > 3.5$), three peaks emerge from the amorphous hump (Fig. 7). The peaks appear at $2\theta = 20.5$, 25.5, and 29°, close to the 2θ values of PET, although the width of the peaks prevents us from affirming that the crystalline parameters are the same. The calculated degree of crystallinity X_c' (18%) is well below the maximum PET X_c' value. This study clearly confirms the appearance of a crystalline phase above a critical draw ratio in drawn PETG but probably with a low degree of crystallinity. We can suppose that above the critical draw ratio, the orientation of the macromolecules is enough to create oriented crystallites. These crystallites did not change the transparency (for visible light) of the material. Optical observations with cross-polarizing plates did not indicate the presence of a crystalline superstructure as spherulites but did show an important birefringence of the material. We

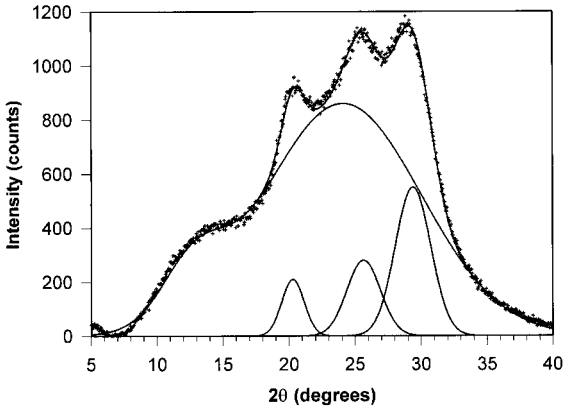

Figure 7 XRD curve for a drawn PETG ($\lambda = 6.4$). Data are the plots and the lines correspond to computer calculations.

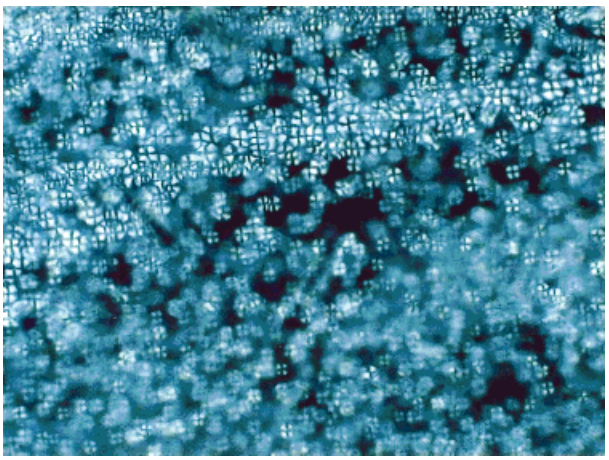

Figure 8 Optical micrographs for an annealed PETG.

can assume that, as in PET, it is because of the small size of the crystallites. Thus, this study confirms previous work on the ability of PETG to crystallize[10] and allows us to propose a second explanation for the DSC baseline perturbations.

For annealed (up to 130°C) drawn PETG, the XRD pattern shows an increase of the area of the three peaks characteristic of a crystalline phase (not shown here). The disappearance of the DSC exothermic peak (Fig. 3) is concomitant with the increase of the apparent degree of crystallinity. As a consequence, we can attribute the exothermic phenomena to a crystallization of a portion of the material. The heating of the drawn sample induced modification in the dimensions of the crystallites. However, because an exotherm was observed for drawn PETG, we can suppose that the crystallinity had not reached its maximum and an extra thermal crystallization is possible during DSC scan. This thermal crystallization probably occurs by growth of the strain-induced crystalline phase, as shown for PET.[24]

If a strain-induced crystalline phase can appear, we can also expect thermal crystallization from the glassy state. Undrawn PETG samples were annealed at 120°C for various times. No crystalline phase appeared during a time below 48 h. For annealing times above 48 h, the samples become opaque and white, suggestive of crystallization. Optical observation (Fig. 8) shows a spherulitic crystallization. The spherulites are small (3 μm radius), indicating that the crystallization acts essentially by nucleation rather than by growth of initial nucleus. The DSC scan (Fig. 9) shows the glass transition and two endothermic melting peaks. The first peak at 144°C is

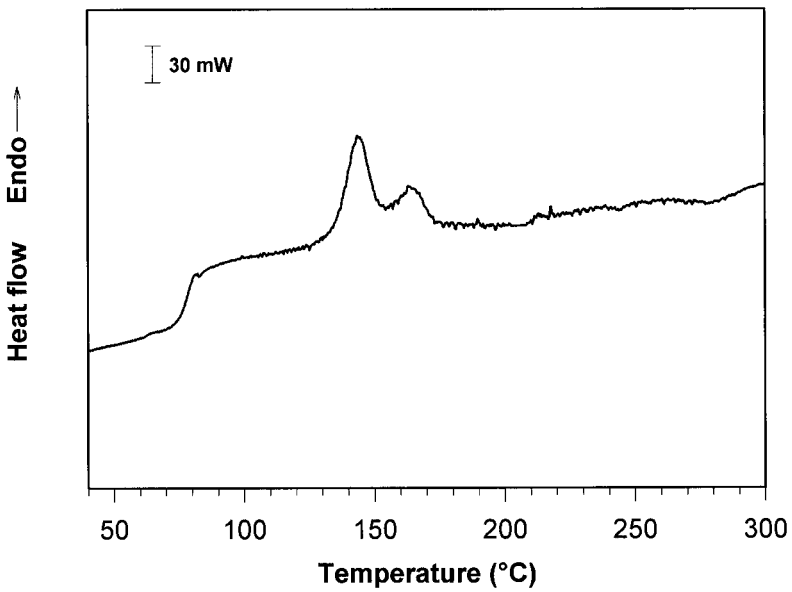

Figure 9 DSC curve for an annealed PETG (6 days at 120°C).

attributed to the annealing and the second at 163°C corresponds to the melting of the nonmodified crystalline phase.

No diffraction peaks are observable by XRD (Fig. 10), although the response of amorphous PETG differentially shows that the broad peak is asymmetric. Computer calculations performed using the shape of the PETG amorphous response (Fig. 4) and the three peaks at the same 2θ values give a low value for X_c' (11%). This can explain, in part, the weakness of the melting enthalpies (8 J g^{-1} K^{-1} for PETG and 39 J g^{-1} K^{-1} for PET). In conclusion, introduction of a second glycol leads to a drastic decrease in the rate of crystallization but did not avoid the appearance of such a phase.

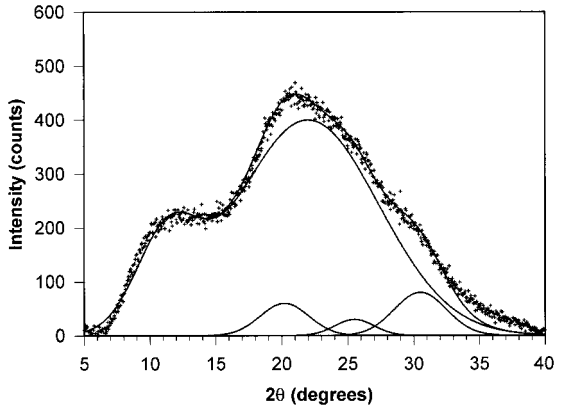

Figure 10 XRD curve for an annealed PETG (6 days at 120°C).

A lengthy annealing allows PETG to crystallize. The spherulitic superstructure is composed of approximately 11% of crystalline phase (27% in the case of PET). From the XRD value, it is possible to calculate ΔH_f° ($\Delta H_f^\circ = \Delta H_f / X_c' = 88$ J/g) and estimate the degree of crystallinity of drawn PETG. Because of the proximity of the two DSC peaks the enthalpy of crystallization is difficult to calculate but is close to 5 J g^{-1} K^{-1}. Thus the initial degree of crystallinity of the highly drawn samples is $X_c = 3\%$. After annealing, the degree of crystallinity of drawn PETG samples can reach 10% of the materials.

CONCLUSIONS

PETG is usually used as amorphous material by the industry because of its very low crystallinity rate. However, the crystalline phase could appear as well by an annealing from the glassy state or by a stretching at high draw ratio. The crystalline rate is very low for the appearance of a crystalline phase from the glassy state by annealing. Even the degree of crystallinity is weak, close to 11%, and the material becomes opaque as a result of the spherulitic superstructure. The SIC phase appears during the drawing but the degree of crystallinity is very weak (3%). This degree of crystallinity is too low to prevent important thermal shrinkage. The crystallites acts as nuclei for a supplementary thermal crystallization, which ap-

pears at a temperature just above the glass-transition temperature. The annealing of SIC material allows the crystalline phase to reach the same degree of crystallinity as that for undrawn annealed material. Nevertheless, some questions are still open. How can this statistical copolyester crystallize? The PETG melting temperature is well below that of PET. Is it the result of a different crystalline lattice structure or of a smaller crystallite size?

REFERENCES

1. Ward, I. M. Text Res J 1961, 31, 650.
2. Dulmage, W. J.; Geddes, A. L. J Polym Sci 1958, 31, 499.
3. Jabarin, S. A. Polym Eng Sci 1992, 32, 1341.
4. Faisant de Champschesnel, J. B.; Bower, D. I.; Ward, I. M.; Tassin, J. F.; Lorentz, G. Polymer 1993, 34, 3763.
5. Cole, K. C.; Guèvremont, J.; Ajji, A.; Pellerin, E.; Dumoulin, M. M. in Proceedings of the Composites '96/Oriented Polymers Symposium, October 9–11, 1996; Boucherville, Canada, 1996.
6. Roland, C. M.; Sonnenschein, M. F. Polym Eng Sci 1991, 31, 1434.
7. Allen, E. O. Plastic Polymer Science and Technology; Wiley: New York, 1982; p. 571.
8. Nabi Saheb, D.; Jog, J. P. J Polym Sci Polym Phys Ed 1999, 37, 2439.
9. Papadopoulou, C. P.; Kalfoglou, N. K. Eur Polym J 1997, 33, 191.
10. Radhakrishnan, S.; Nadkarni, V. M. Eur Polym J 1986, 22, 67.
11. Hwang, S. H.; Jeong, K. S.; Jung, J. C. Eur Polym J 1999, 35, 1439.
12. Seyler, R. J. J Therm Anal 1997, 49, 491.
13. Quintanilla, L.; Rodriguez–Cabello, J. C.; Jawhari, T.; Pastor, J. M. Polymer 1993, 34, 3787.
14. Tan, S.; Su, A.; Li, W.; Zhou, E. J Polym Sci Polym Phys Ed 2000, 38, 3787.
15. Elenga, R.; Seguela, R.; Riestsch, F. Polymer 1991, 32, 1975.
16. Turi, E. A. Thermal Characterization of Polymeric Materials; Academic Press: New York, 1981; p. 721.
17. Gruenwald, G. Plastics: How Structure Determines Properties; Hanser: Munich, 1993; p. 142.
18. Dargent, E.; Denis, G.; Caron, C.; Saiter, J. M.; Grenet, J. J Appl Polym Sci to appear.
19. Rietsch, F. Eur Polym J 1990, 10, 1077.
20. Dargent, E.; Grenet, J.; Auvray, X. J Therm Anal 1994, 41, 1409.
21. Daubeny, R. de P.; Bunn, C. W.; Brown, C. J. Proc R Soc London A 1954, 226, 531.
22. Dargent, E.; Grenet, J.; Dahoun, A. Polym Eng Sci 1997, 37, 1853.
23. Wunderlich, B. Macromolecular Physics, Vol. 3; Academic Press: New York, 1980.
24. Dargent, E.; Denis, A.; Galland, C.; Grenet, J. J Therm Anal 1996, 46, 377.